

ZoneFlow™-Bayonet Steam Reforming Reactor for the Purposes of Reduced Firing and Zero to Negative Steam Export:

Pressure Drop and Heat Transfer Modelling and Evaluation of the Reactor Performance

Juray De Wilde, Luis Calamote de Almeida, Jonathan Feinstein, Florent Minette

Materials & Process Engineering (IMAP), Université catholique de Louvain (UCLouvain), Place Sainte
Barbe 2, B-1348 Louvain-la-Neuve, Belgium, juray.dewilde@uclouvain.be

Research and Innovation Centre for Process Engineering (ReCIPE), Place Sainte Barbe 2, B-1348
Louvain-la-Neuve, Belgium

ZoneFlow Reactor Technologies, LLC, Windsor, CT, USA

Abstract:

The ZoneFlow™ reactor is an annular structured reactor that offers lower pressure drop and significantly better heat transfer than standard pellets used in Steam Methane Reforming. An annular structured casing is suspended on a central tube equipped with discs, ensuring close contact between the casing and the reactor tube wall. The annular ZoneFlow™ reactor is particularly suited for use in a bayonet configuration. The produced syngas then returns via the central tube, the so-called bayonet, allowing counter-current heat exchange between the return gas and the gas reacting in the ZoneFlow™ reactor, referred to as reacting gas. To intensify the heat transfer between the gas in the bayonet and in the annulus, an insert is installed inside the bayonet, forming a second annulus that forces the gas to flow close to the bayonet wall at high velocity. In the present work, the pressure drop

and heat transfer resulting from various bayonet configurations are experimentally measured at commercial scale reactor dimensions and air flow rates equivalent to commercial conditions. Correlations for the friction factors and the heat transfer coefficients are derived from the data. The correlations are then used to simulate a commercial scale ZoneFlowTM-bayonet reactor and optimize the design.

Keywords: Steam Methane Reforming; Heat recovery; Structured reactor; Pressure drop; Heat transfer.

1. Introduction

Steam Methane Reforming (SMR) is one of the most widely used processes for the production of hydrogen and syngas ($\text{CO} + \text{H}_2$). The reactions are strongly endothermic and a multi-tubular fixed bed reactor is used with hundreds of small diameter (ca. 0.1 m) tubes packed with relatively large catalyst pellets suspended in a furnace. Because of chemical equilibrium limitations, high methane conversion requires a high gas exit temperature approaching 900°C. Heat recovery from the syngas that leaves the reactor at maximum temperature is conventionally achieved by steam generation downstream of the reforming reactors. The steam is used in the SMR process itself, but unwanted, low value excess steam is also typically and unavoidably produced. Bayonet reactors integrate heat recovery to use the heat from the syngas directly in the reforming reactions. This has several potential advantages. First, for a given capacity, less firing and less tubes are required, and a smaller furnace plot can be used. Natural gas consumption and related CO_2 emissions are projected to decline 5% [Air Liquide, 2020]. More importantly, syngas exits the tube at a lower temperature, excess steam production is eliminated, and the process boiler is eliminated for increased plant reliability. Bayonet reactors are an effective form of integrated heat recovery. Instead of using a straight-through reactor tube, the reactor tube is closed at its bottom end and the syngas is forced to return and exit via an inner tube, the so-

called bayonet, centrally installed within the reactor or outer tube. Heat exchange is counter-current between the reacting gas, previously in a packed bed, and the return gas in the bayonet such that the return gas leaves the top of the bayonet, i.e. the same end as the reactor inlet, at a reduced temperature. Thirdly, a bayonet reactor simplifies the reactor suspension system as the reactor tube can freely elongate and contract without straining the inlet and outlet connections. The recently introduced SMR-b [Haldor Topsoe, 2020] and SMR-XTM [Saudemont, 2018; Air Liquide, 2020] technologies are bayonet reactor based. Bayonet heat exchanger type reactors have been considered for other applications as well, such as for sulfuric acid decomposition in thermochemical hydrogen production processes [Corgnale et al., 2017] and for steam generation for lead-cooled fast nuclear reactors (LFR) [Damiani et al., 2013]. The use of a bayonet tube with packed beds famously increases pressure drop – first, because the reactor cross section is reduced to only a portion of the tube cross section and, secondly, because return gas must change flow direction and then travel the same distance in reverse through the remaining portion of the tube cross section. The pressure drop mainly occurs in the annular packed bed in tubes where increased diameter would only lower the ratio of heat transfer surface area-to-reactor volume in a heat transfer constrained process. Further, the ratio of particle size-to-annulus width invites bypass and more pronounced wall effects. Although low-pressure drop, high-voidage pellets could be used to limit the pressure drop, this is limited by the crushing strength of the pellets and is detrimental to heat transfer.

The inherently flexible annular structured reactor packing of ZoneFlow Reactor Technologies (ZFRT), LLC, provides improved heat transfer compared to conventional pellets at comparable or lower pressure drop, using a narrower annulus without bypass or failure due to crushing than is feasible with pellets [De Wilde and Froment, 2012; 2013; Minette et al., 2021]. The narrower annulus in the ZoneFlowTM design permits use of a larger inner tube with several times greater heat transfer surface area than in a bayonet reactor with pellets [Ralston and Feinstein, 2015]. The purpose of the present work is to generalize and optimize the intensification of heat transfer between the reacting gas and the return gas.

2. The ZoneFlow™-bayonet reactor

The ZoneFlow™ reactor is an annular structured reactor that improves pressure drop and heat transfer compared to standard pellets used in SMR [Minette et al., 2021]. The annulus is 14 mm wide (in the radial direction) and the structured casing is circumferentially divided into columns separated from one another by radial walls. Alternating columns guide the flow towards and away from the reactor tube wall, respectively, by means of blades at a 45° angle to the vertical axis and that together with the radial walls form slanted rectangular channels (Figure 1a). Flow from one column to the next is only possible near the walls, via openings in the radial walls. Short cylindrical spacers and discs to hold the casings in place slide down around the central, continuous, gas tight, metal dusting resistant bayonet tube. A gap of approximately 50 µm is observed between the sliding cylindrical spacers and the bayonet tube. The casings are in the form of cylindrical bands that are stacked (Figure 1b). Each column of each casing contains six oblique blades from top to bottom (Figure 1a). The casings are wrapped around stacks of spacers and discs to form a module and the modules slide into position down the central tube. The blades are evenly spaced at 17 mm top-to-top in the 100 mm long casings. Midway from ID to OD, the columns are circumferentially 5.9 mm wide, resulting in an average hydraulic channel diameter of 8.8 mm. Two to four discs hold each casing in place, depending on the desired tradeoff between heat transfer and pressure drop for a given plant (Figure 1c with two discs). Gravity and the flow push the 45° angle blades onto the discs, moving the casings radially outward and ensuring close contact between the casings and the reactor tube wall.

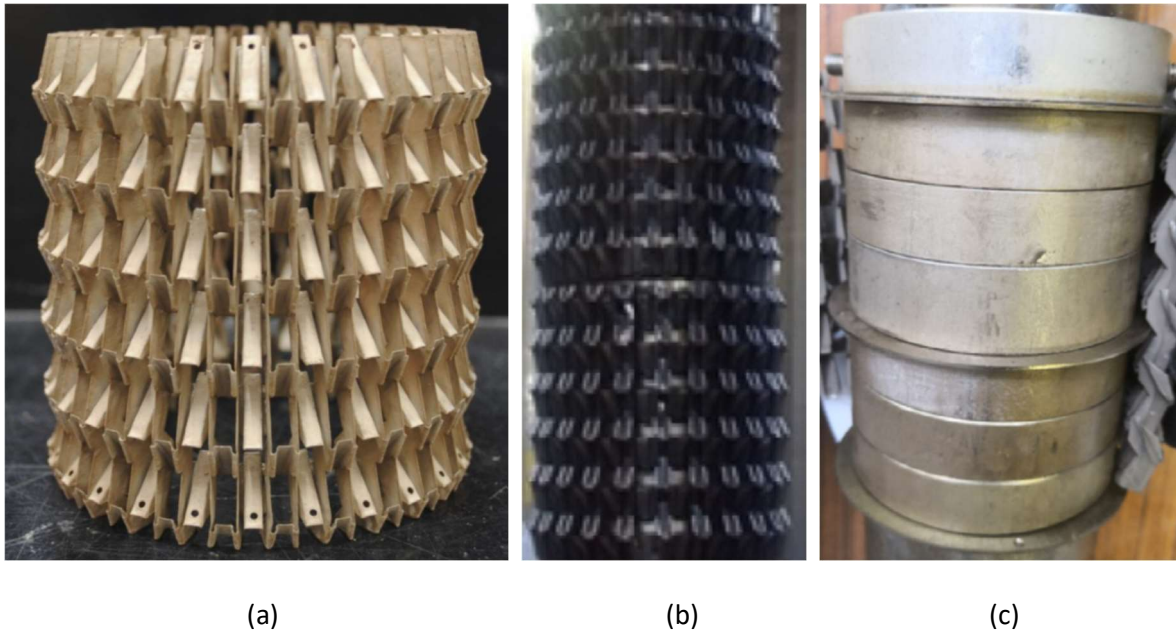


Figure 1. (a) Structured ZoneFlow™ reactor casing; (b) Two stacked casing elements; (c) Central support tube and spacers with 2 discs per casing element.

The annular ZoneFlow™ reactor is particularly suited for use with a bayonet tube for heat recovery, but flow through an empty bayonet is low velocity resulting in insignificant heat transfer. A closed tube or plug of a specified length is inserted into the bayonet tube to form a second annulus (Figure 2), near the reactor inlet / bayonet exit end where the temperature difference or driving force for heat transfer between the reactor annulus and return gases is the most pronounced. The return gas in the bayonet is forced through a short annulus, causing high velocity close to the bayonet wall to intensify heat transfer with the latter. The diameter and length of the insert are discussed later in this paper.

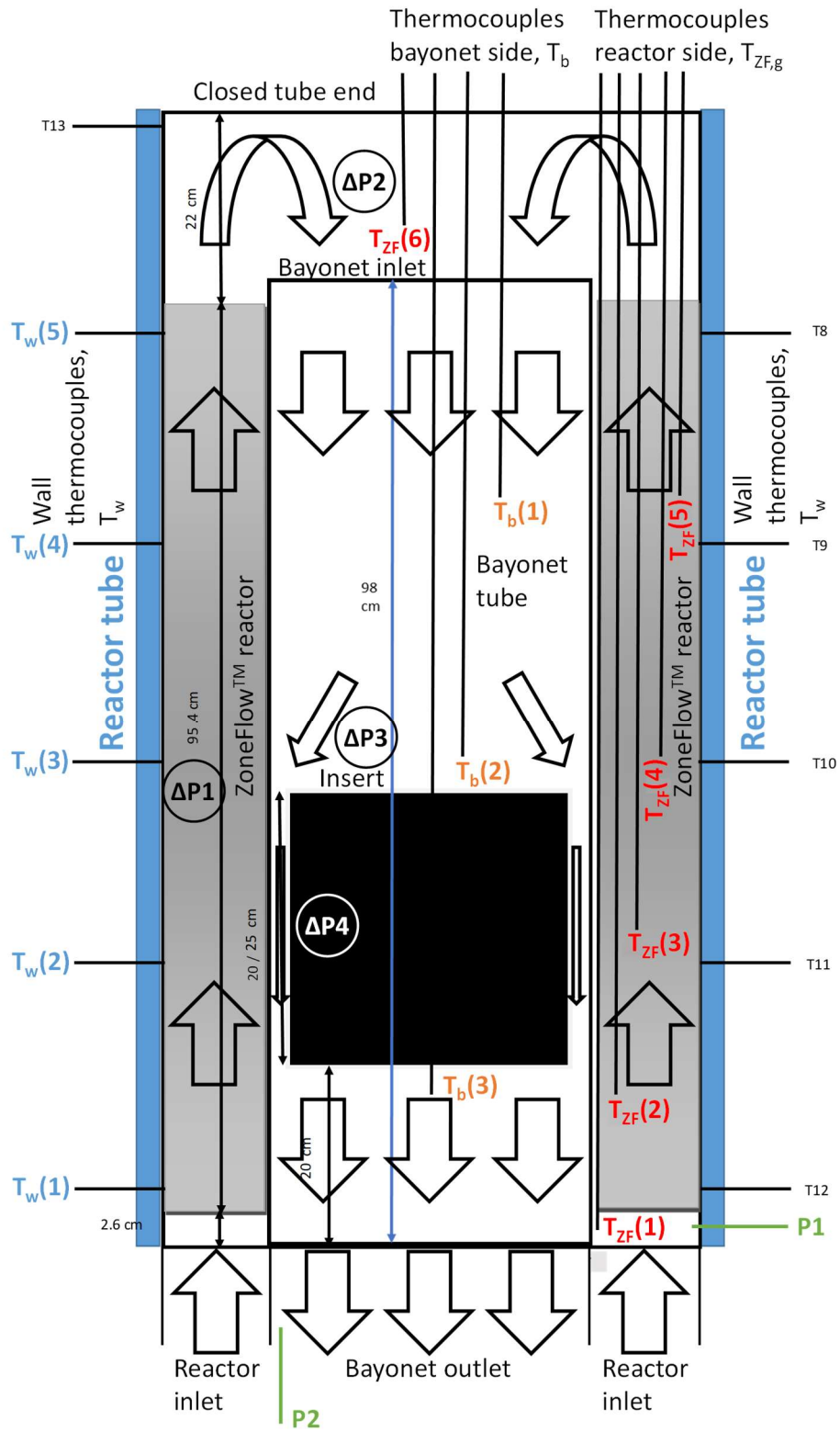


Figure 2. Schematic drawing of the ZoneFlow™-bayonet reactor with the bayonet insert as used in the experimental study.

3. Pressure drop and heat transfer modelling

For the ZoneFlow™ reactor, the pressure drop and heat transfer between the inside of the reactor tube and the reacting gas was previously measured, and correlations for the friction factor and for the heat transfer coefficient were derived from the experimental data [Minette et al., 2021]. The present work focuses on the pressure drop in the bayonet with inserts and the heat transfer between the reacting gas and the return gas in the bayonet without and with inserts of various lengths.

3.1. Pressure drop modelling

Pressure drop is distinguished between four contributing flow regions (Figure 2). The first is the pressure drop in the annular structured ZoneFlow™ reactor, ΔP_1 , which has been previously measured and modeled [Minette et al., 2021]. A second contribution, ΔP_2 , is the pressure drop at the tip between the outlet of the reactor annulus and the inlet of the bayonet tube, where the flow abruptly changes direction. The pressure drop in the empty bayonet tube itself, that is, in the region without insert, is found to be negligible. The third contribution is the pressure drop at the inlet of the bayonet insert, ΔP_3 , and the fourth pressure drop is along the length of the annulus between the bayonet wall and the insert, ΔP_4 . Data with inserts of different lengths allow distinction to be made between the third and fourth contributions.

For the pressure drop in the annular ZoneFlow™ reactor (ZF14mm-2D design), ΔP_1 , Minette et al. [2021] adopted the Fanning equation based on the similarity with flow through a bundle of empty channels:

$$\Delta P_1 = \int_0^{L_{ZF}} 2f \frac{\rho_g u_s^2}{d_{h,ZF}} dz \quad (1)$$

with $d_{h,ZF}$ the average hydraulic diameter of an oblique ZoneFlow™ casing channel (8.8 mm), L_{ZF} the total length of the ZF packing, and:

$$f = \frac{16}{Re_{d_{h,ZF}}} + a_1 Re_{d_{h,ZF}}^{-a_2} \quad (2)$$

where $Re_{d_{h,ZF}} = Gd_{h,ZF}/\mu$. The parameters $a_1 = 0.401$ and $a_2 = 0.07$ were experimentally determined. The pressure drop in the highly turbulent region between the ZoneFlow™ reactor outlet and the bayonet inlet, ΔP_2 , is correlated as a local pressure drop according to:

$$\Delta P_2 = K_2 \frac{\rho_g u_s^2}{2} \quad (3)$$

where it was chosen to use the superficial velocity at the outlet of the ZoneFlow™ reactor for u_s and K_2 is the local loss coefficient to be experimentally determined from the measurements without a bayonet insert. Similarly, the pressure drop related to the inlet effect of the bayonet insert is described as:

$$\Delta P_3 = K_3 \frac{\rho_g u_{s,b}^2}{2} \quad (4)$$

where $u_{s,b}$ is the superficial velocity in the bayonet tube, i.e. with no insert, and K_3 is the local loss coefficient determined from the measurements with bayonet inserts of different lengths.

For the pressure drop along the annulus between the bayonet insert and the bayonet wall, a Darcy-Weisbach-type relation was adopted:

$$\Delta P_4 = \int_{L_{bi}^0}^{L_{bi}} 2f_{bi} \frac{\rho_g u_{s,bi}^2}{d_{h,bi}} dz' \quad (5)$$

where $u_{s,bi}$ is the velocity in the above specified annulus and $d_{h,bi}$ is the hydraulic diameter of this annulus, $d_{h,bi} = d_{b,in} - d_{bi} = 3.75 \text{ mm}$, which is twice the annulus width. The friction factor, f_{bi} , is correlated by:

$$f_{bi} = a_3 Re_{d_{h,bi}}^{-a_4} \quad (6)$$

where $Re_{d_{h,bi}} = \rho_g u_{s,bi} d_{h,bi} / \mu$. Three parameters, K_3 , a_3 and a_4 were estimated by regression from the experiments with bayonet inserts of different lengths. The objective function is:

$$SSQ = \sum_{i=1}^n (\Delta P_i - \widehat{\Delta P}_i)^2 \quad (7)$$

where ΔP_i and $\widehat{\Delta P}_i$ are the measured and predicted pressure drop for the i^{th} experiment. Athena Visual Studio was used for the parameter estimation.

3.2. Heat transfer modelling

It was postulated by simple calculations that in the experimental set-up heat transfer between the reacting gas and the return gas in the bayonet only takes place along the length of the insert. Temperature measurements confirmed that heat transfer in the empty bayonet tube is indeed negligible. Focusing on the heat transfer in the region with the bayonet insert, the global heat transfer coefficient for heat transfer between the return gas in the bayonet and the reacting gas, $U_{b,ZF}$, consists of three contributions. From the added resistances theory:

$$\frac{1}{U_{b,ZF}} = \frac{1}{\alpha_{b,in}} + \frac{A_{b,in}}{A_{b,m}} \frac{t_{bw}}{\lambda_{bw}} + \frac{A_{b,in}}{A_{g,m}} \frac{t_g}{\lambda_{air}} + \frac{A_{b,in}}{A_{s,m}} \frac{t_{sw}}{\lambda_{sw}} + \frac{A_{b,in}}{A_{b,ZF}} \frac{1}{\alpha_{b,ZF}} \quad (8)$$

where $\alpha_{b,in}$ is the coefficient of heat transfer between the inside of the bayonet tube and the return gas in the bayonet in the region with insert, t_{bw} and t_{sw} are the bayonet tube and sliding spacers thicknesses, t_g is the air gap between the bayonet tube and the sliding spacers, λ_{bw} and λ_{sw} are the thermal conductivity of the bayonet tube itself and the sliding spacers (25 W/m/K) and $\alpha_{b,ZF}$ is the coefficient of heat transfer between the outside of the bayonet tube and the reacting gas. For $\alpha_{b,in}$, the correlation of Dittus-Boelter [1930] for turbulent cooling flow in concentric annuli was adopted:

$$Nu_{b,in} = \frac{\alpha_{b,in} d_{h,bi}}{\lambda_g} = 0.023 Re_{d_{h,bi}}^{0.8} Pr^{0.4} \quad (9)$$

The applicability of the Dittus-Boelter correlation was verified by means of Computational Fluid Dynamics (CFD) simulations, presented in Appendix I. This left the correlation for $\alpha_{b,ZF}$ to be experimentally determined, requiring measurements of the temperature profiles in the ZoneFlow™

reactor, $T_{ZF,g}$, and in the bayonet, T_b . Based on the similarity of the flow in the structured ZoneFlow™ reactor with flow through a bundle of empty channels, $\alpha_{b,ZF}$ is correlated to be:

$$Nu_{b,ZF} = \frac{\alpha_{b,ZF} d_{h,ZF}}{\lambda_g} = \frac{\alpha_{b,ZF}^0 d_{h,ZF}}{\lambda_g} + b_1 Re_{d_{h,ZF}}^{b_2} Pr^{0.33} \quad (10)$$

In Eq. (10), $\alpha_{b,ZF}^0$ is the static contribution to the heat transfer coefficient in the ZoneFlow™ structured packing, which can be defined as:

$$\alpha_{b,ZF}^0 = \frac{\lambda_{er,ZF}^0}{\Delta r_{ZF}} \quad (11)$$

with $\lambda_{er,ZF}^0$ the effective radial thermal conductivity in the reactor with packing and Δr_{ZF} the ZoneFlow™ reactor annulus width. Accounting for the packing void fraction and thickness of the metal sheet used, $t_{ZF} = 100 \mu m$, Minette et al. [2021] derived:

$$\frac{\lambda_{er,ZF}^0}{\lambda_g} = \varepsilon + \frac{(1-\varepsilon)}{212 t_{ZF} + 2.82 \frac{\lambda_g}{\lambda_s}} \quad (12)$$

The parameters b_1 and b_2 in Eq. (10) are estimated by regression imposing the measured values of the temperature in the ZoneFlow™ reactor, $T_{ZF,g}$, and of the temperature in the bayonet immediately upstream of the insert region, $T_b(2)$, and integrating the energy equation on the bayonet side where the insert is located:

$$u_{s,bi} \rho_g c_P \frac{dT_b}{dz'} = A_{b,in} U_{b,ZF} (T_{ZF,g} - T_b) \quad (13)$$

The specific heat exchange surface area inside the bayonet in the region of the insert, $A_{b,in}$, is $549.5 m_{b,in}^2 / m_{bi}^3$. The parameters are optimized to fit the measured temperature in the bayonet immediately downstream of the insert region, $T_b(3)$, so that the objective function is:

$$SSQ = \sum_{i=1}^n (T_b(3)_i - \widehat{T_b(3)_i})^2 \quad (14)$$

Athena Visual Studio was used for the parameter estimation.

4. Experimental set-up

The experimental set-up consists of an air compressor, a mass flow controller for the air flow rate, the ZoneFlow™-bayonet reactor installed in a reactor tube, suspended in a furnace, the required pressure sensors and thermocouples, and the air vent line. The reactor tube has an OD of 0.108 m, an ID of 0.10 m, and is 1.2 m long, of which 1 m is heated inside the electrical furnace. The bayonet tube on which the casing elements are suspended has an OD of 0.072 m and an ID of 0.06375 m. This leaves a 14 mm wide annulus in which ZoneFlow™ casing elements are stacked over a length of 0.954 m. The reactor tube and bayonet tube diameters are of commercial scale. The bayonet inserts that were used have an OD of 0.06 m and a length of either 0.2 m or 0.25 m. The bayonet insert is mounted near the exit of the bayonet. Reference tests in the absence of an insert were also carried out. The ZoneFlow™ reactor and bayonet dimensions are summarized in Table 1. For practical reasons, the experimental set-up operates with up-flow in the ZoneFlow™ reactor and down-flow in the bayonet tube, the opposite of industrial practice.

ZoneFlow™ length	L_{ZF}	95.4 cm
ZoneFlow™ annulus width	Δr_{ZF}	14 mm
ZoneFlow™ hydraulic diameter	$d_{h,ZF}$	8.8 mm
ZoneFlow™ tube OD	d_{ZFto}	10.8 cm
ZoneFlow™ tube ID	d_{ZFti}	10 cm
Sliding spacer OD	d_s	7.2 cm
Bayonet insert length	L_{bi}	20-25 cm
Bayonet tube ID	$d_{b,in}$	6.375 cm
Bayonet insert OD	d_{bi}	6 cm
Bayonet hydraulic diameter	$d_{h,bi}$	0.375 cm
Air gap between bayonet tube and sliding spacer	t_g	50 μm

Table 1. Dimensions of the ZoneFlow™-bayonet reactor used in the experimental study.

The air flow rate is set by means of a mass flow controller and was varied between 70 and 237 Nm³/h, with a Reynolds number range relevant for commercial scale Steam Methane Reforming [Minette et al., 2021]. In the pressure drop tests, the pressure is only measured at the inlet of the reactor and at the outlet of the bayonet, as the pressure drop over the annular ZoneFlowTM reactor is known from previously measured data [Minette et al., 2021]. The pressure drop between the reactor outlet and the bayonet inlet was measured from the tests without a bayonet insert, since the pressure drop in the empty bayonet is negligible. By testing with the bayonet inserts of different lengths, the insert inlet pressure drop and the pressure drop along the length of the annulus between the insert and the bayonet wall were determined. In the respective heat transfer tests, the furnace temperature over the length of the furnace was set to 300, 400 and 500°C. As shown in Figure 2, the reactor tube wall temperature, T_w , was measured at 5 axial positions. To shield these thermocouples from radiation, they were cemented 2 mm deep inside the 4 mm thick tube wall. The air temperature was measured at the inlet of the annular reactor containing the ZoneFlowTM structured packing and at 5 axial positions inside the annular reactor, indicated by $T_{ZF,g}$ in Figure 2. Finally, the air temperature in the bayonet, T_b , was measured at three axial positions, first in the empty bayonet, just prior to entering the insert, and just downstream of the insert. A picture of the experimental set-up is shown in Figure 3.

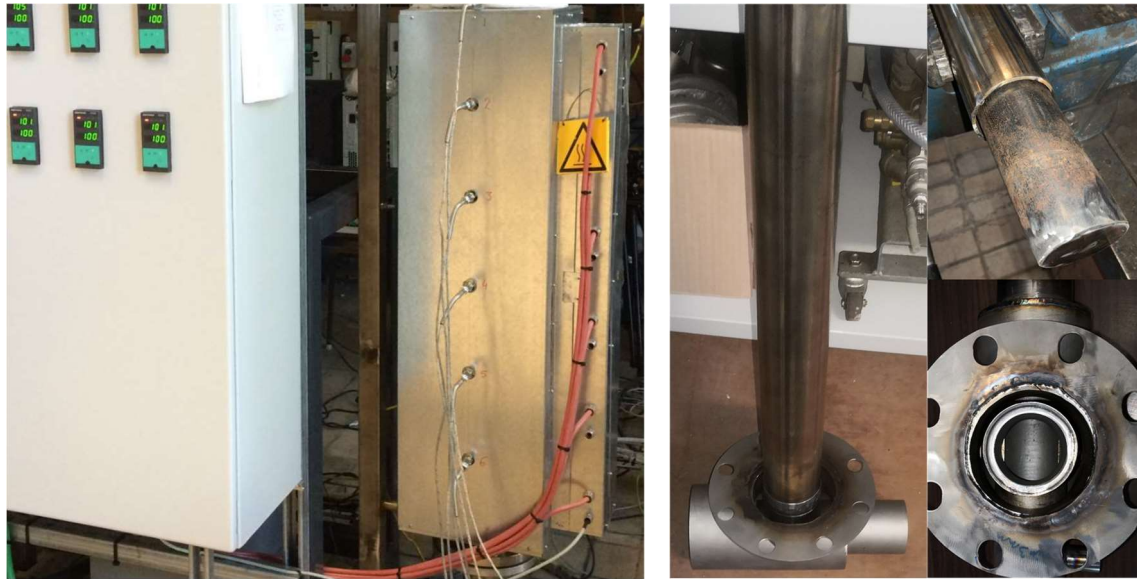
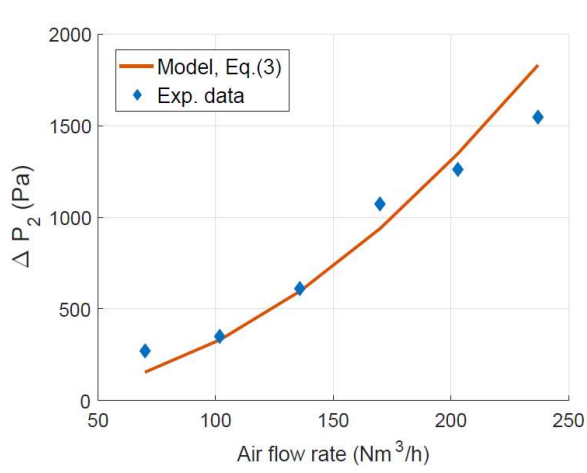


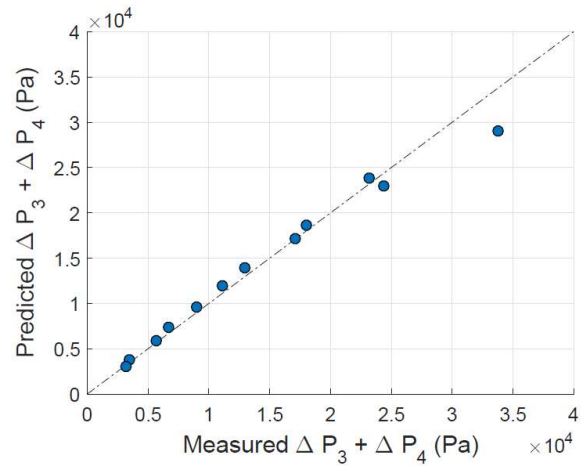
Figure 3. Pictures of the experimental set-up to study the pressure drop and heat transfer of the ZoneFlow™-bayonet reactor (left) and of the bayonet, the bayonet insert and the reactor inlet / bayonet exit (right).

5. Experimental results and parameter estimation

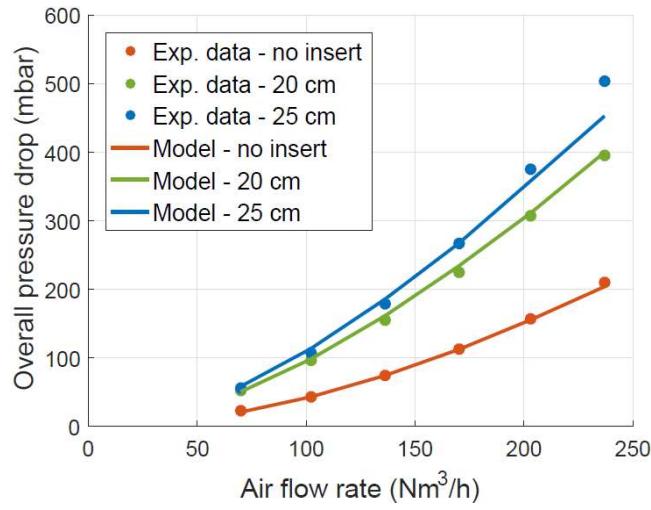
The pressure drop measurements without a bayonet insert allowed determination of $K_2 = 8.33$, see Eq. (3), for the pressure drop in Pa. The fit between the experimental data and model predictions for ΔP_2 is shown in Figure 4a. From the pressure drop measurements with bayonet inserts of different lengths, the values of the parameters, K_3 , a_3 and a_4 in Eqs. (4) and (6) were estimated. The values and 95% confidence intervals are summarized in Table 2.



(a)



(b)



(c)

Figure 4. Pressure drop measurements and model predictions for the ZoneFlow™-bayonet reactor.

(a) ΔP_2 measured in the absence of a bayonet insert, Eq. (3); (b) Over the bayonet ($\Delta P_3 + \Delta P_4$), Eqs. (4)-(6); (c) Overall pressure drop in the absence of a bayonet insert or with a 20 or 25 cm-long bayonet insert. Dimensions: see Table 1.

Parameter	Value \pm 95% confidence interval	t-value
Pressure drop		
K_2	8.33	
K_3	9.538 ± 3.73	5.65
a_3	0.062 ± 0.003	46.27
a_4	-0.23 ± 0.0045	112.2
Heat transfer		
b_1	1.98 ± 0.66	6.31
b_2	0.47 ± 0.041	23.94

Table 2. Experimentally determined parameter values and 95% confidence intervals for the pressure drop and heat transfer correlations.

Note that Quarmby [1967a;b] found for the pressure drop in concentric annuli $a_3 = 0.0844$ and $a_4 = -0.255$, which is in relatively good agreement with the values $a_3 = 0.062$ and $a_4 = -0.23$ found in this work. The parity plot in Figure 4b illustrates the agreement between the measured and predicted pressure drop over the bayonet, i.e. $\Delta P_3 + \Delta P_4$, whereas Figure 4c shows the comparison between the measured and predicted overall pressure drop versus air flow rate, with no insert in the bayonet and with an insert either 0.2 or 0.25 m long. Figure 5 shows the pressure versus position profiles in the experimental ZoneFlowTM-bayonet reactor at air flow rates of 102 and 170 Nm³/h, and for the two tested bayonet insert lengths.

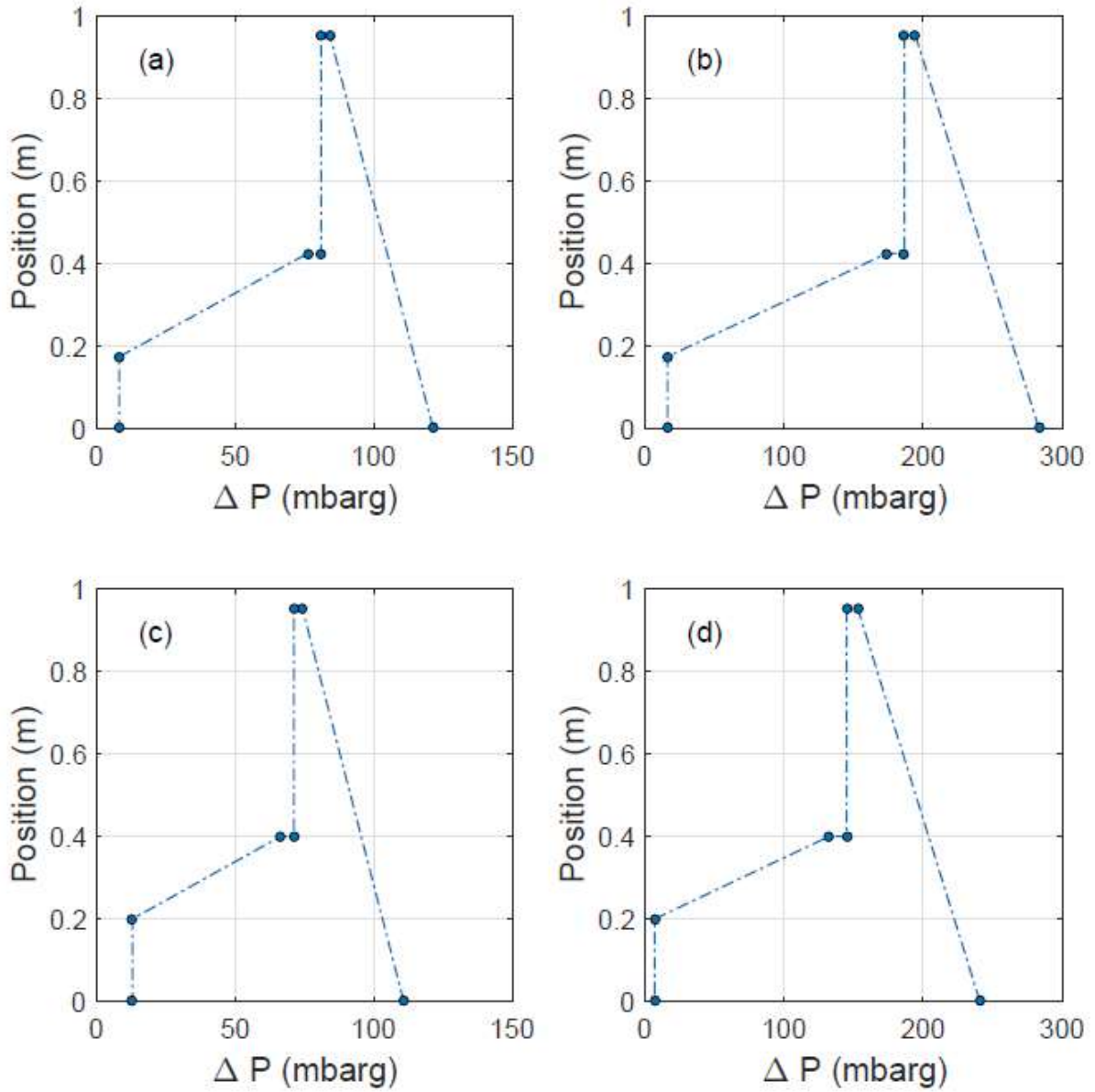


Figure 5. Pressure-position profiles in the experimentally tested ZoneFlow™-bayonet reactor. (a,b) With a 25 cm-long bayonet insert and (c,d) with a 20 cm-long bayonet insert at air flow rates of (a,c) 102 Nm³/h and (b,d) 170 Nm³/h. Dimensions: see Table 1.

Figure 5 also illustrates the relative impacts of ΔP_1 , ΔP_2 , ΔP_3 and ΔP_4 . With the bayonet inserts used leaving a gap of only 1.875 mm between the insert and the bayonet wall, the pressure drop over the length of the insert, ΔP_4 , is the largest, followed by that over the ZoneFlow™ reactor, ΔP_1 . The contribution due to the change in flow direction between the ZoneFlow™ reactor outlet and the

bayonet inlet, ΔP_2 , and the inlet effect of the bayonet insert, ΔP_3 , are relatively small. It should be noted that the pressure drop along the length of the insert, ΔP_4 , is acceptable in combination with the low pressure drop in the ZoneFlow™ reactor itself, ΔP_1 , compared to the pressure drop in conventional pellet reactors [Minette et al., 2021]. The total pressure drop over the ZoneFlow™-bayonet reactor, $\Delta P_1 + \Delta P_2 + \Delta P_3 + \Delta P_4$, is in fact comparable to the pressure drop over a packed bed reactor with conventional SMR catalyst pellets in the absence of a bayonet. Further, a bayonet reactor displaces or eliminates the pressure drops otherwise experienced in the mixed feed preheat, pre-reformer, mixed feed reheat, the longer reformer inlet and outlet goose necks, the process gas boiler, and all interconnect piping.

Note that the bayonet insert used in the experimental tests aimed at minimizing the resistance for heat transfer between the return gas and the inside of the bayonet and measuring heat transfer between the reacting gas and the outside of the bayonet, which had not been previously studied. Later in this work, the insert diameter and length were optimized in terms of heat transfer-pressure drop tradeoffs. The optimized insert design is then used to simulate the performance of a commercial scale ZoneFlow™-bayonet reactor for Steam Methane Reforming.

The heat transfer parameters b_1 and b_2 in Eq. (10) for $\alpha_{b,ZF}$ are estimated from the measurements of the axial profiles of the temperature in the ZoneFlow™ reactor, $T_{ZF,g}$, and in the bayonet, T_b . Values of the parameters and their 95% confidence intervals are given in Table 2. Figure 6 shows the experimentally measured $T_{ZF,g}$ and T_b for the three tested furnace temperatures (300, 400 and 500°C) and for two of the tested air flow rates. Predictions using Eq. (10) with the above reported parameter values are also shown in the region with the bayonet insert, showing good agreement. It is clear from the temperature profiles in Figure 6 that heat is effectively recovered from the return gas exiting through the bayonet, and especially in the region with the bayonet insert.

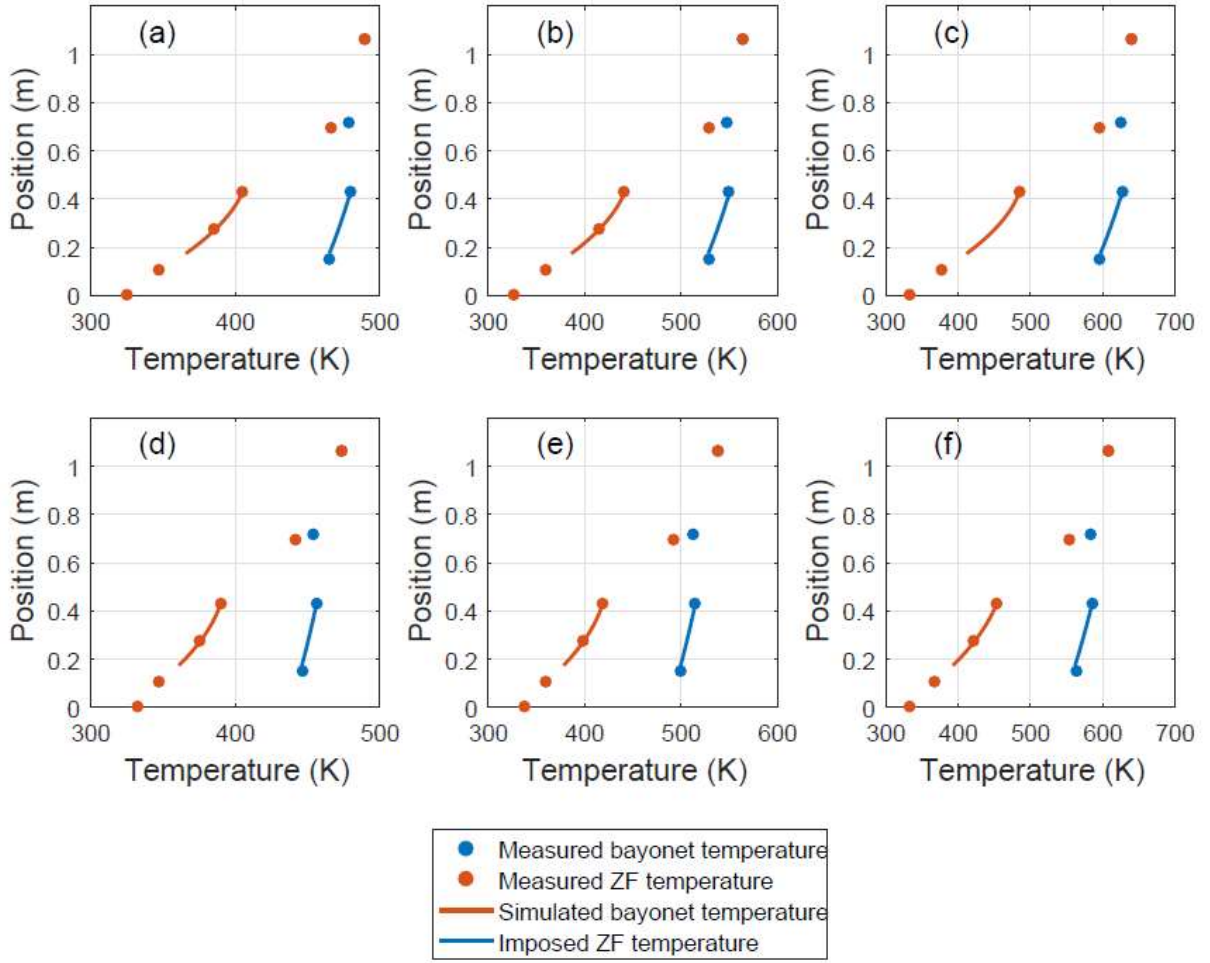


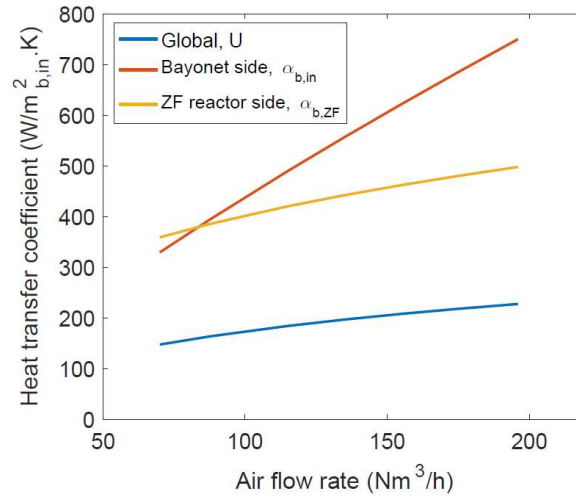
Figure 6. Experimentally measured and calculated temperature profiles in the experimentally studied ZoneFlow™-bayonet reactor with a 25 cm-long bayonet insert, for air flow rates of (a,b,c) 115 Nm³/h and (d,e,f) 175 Nm³/h and for a furnace temperature of (a,d) 300°C, (b,e) 400°C and (c,f) 500°C. Dimensions: see Table 1.

Figure 7a compares the global coefficient of heat transfer between the return gas in the insert region of the bayonet and the reacting gas, $U_{b,ZF}$ in Eq. (8), with the individual contributing heat transfer coefficients, $\alpha_{b,ZF}$ and $\alpha_{b,in}$. The corresponding thermal resistances are shown in Figure 7b. Values are shown as functions of the air flow rate for the conditions summarized in Table 3. Global heat transfer coefficients between 130 and 225 W/m²/K were obtained. With the very narrow bayonet annulus tested, the main resistance to heat transfer between the return gas in the bayonet and the

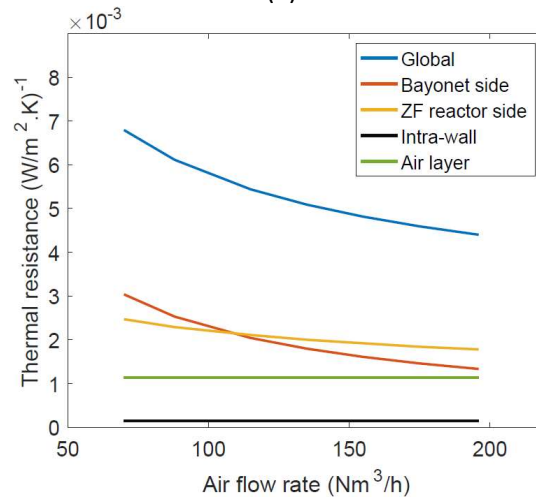
reacting gas is clearly located on the ZoneFlow™ reactor side. This allows a more accurate measurement of the coefficient of heat transfer between the reacting gas and the outside of the bayonet, $\alpha_{b,ZF}$, and the parameters in Eq. (10). The optimal bayonet insert design is derived using the experimentally determined pressure drop and heat transfer correlations, as discussed hereafter. A comparison can also be made between $\alpha_{b,ZF}$ and of the coefficient of heat transfer between the reacting gas and the inside of the reactor tube, $\alpha_{w,ZF}$, previously derived by Minette et al. [2021]:

$$Nu_{ZF} = \frac{\alpha_{w,ZF} d_{h,ZF}}{\lambda_g} = \frac{\alpha_{w,ZF}^0 d_{h,ZF}}{\lambda_g} + 5.38 Re_{d_{h,ZF}}^{0.41} Pr^{0.33} \quad (15)$$

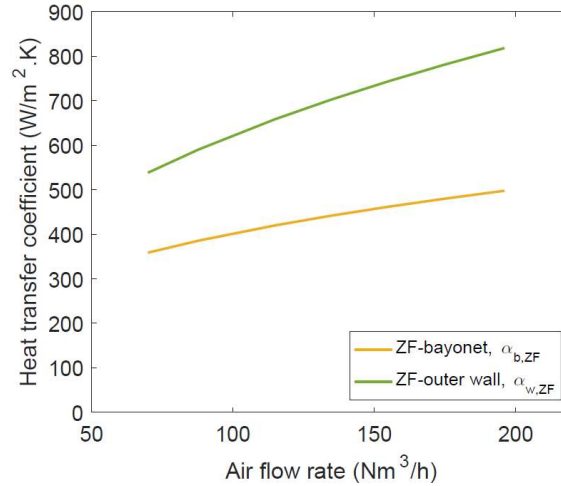
Figure 7c shows that, with two discs supporting each casing element, the reacting gas exchanges heat as efficiently with the inside of the reactor tube as with the outside of the bayonet. The values of $\alpha_{b,ZF}$ are around double of the typical values of the heat transfer coefficient in packed beds of pellets [Minette et al., 2021].



(a)



(b)



(c)

Figure 7. Contributions to the heat transfer between the return gas in the bayonet insert region and the reacting gas for the experimentally tested design: (a) heat transfer coefficient and (b) thermal resistance. (c) Comparison of the heat transfer of the reacting gas with the inside of the reactor tube and with the outside of the bayonet. Dimensions: see Table 1. Air properties and conditions: see Table 3.

Temperature, T	300°C
Pressure, p	1 bar
Viscosity, μ	$3 \times 10^{-5} \text{ Pa.s}$
Heat capacity, c_p	1027 J/kg.K
Thermal conductivity, λ_g	0.044 W/m.K
Prandtl number, Pr	0.7

Table 3. Air properties and operating conditions used to evaluate of the various resistances to heat transfer in the ZoneFlow™-bayonet reactor.

6. Simulation of a commercial scale steam methane reformer using the ZoneFlow™-bayonet reactor and optimization of the bayonet insert design

The coupled reactor-bayonet simulations with the reactions use a steady state 1D model [Froment et al., 2010]. A heterogeneous model is used for the ZoneFlow™ reactor side to account for interfacial heat and mass transfer limitations and intra-catalyst mass transport limitations. The gas and solid phase species continuity and energy equations in the ZoneFlow™ reactor are:

$$\frac{d(u_s C_A)}{dz} = k_{gs} a_{gs,ZF} (C_{A,s}^s - C_A) \quad (16)$$

$$k_{gs} (C_{A,s}^s - C_A) = \sum_j \alpha_{A,j} \eta_j t_{ZF,c} \rho_s r_j(C_s, T_{ZF,s}) \quad (17)$$

$$u_s \rho_g c_p \frac{dT_{ZF,g}}{dz} = h_{gs} a_{gs,ZF} (T_{ZF,s} - T_{ZF,g}) + \alpha_{w,ZF} a_{w,in} (T_w - T_{ZF,g}) + U_{b,ZF} \hat{A}_{b,in} (T_b - T_{ZF,g}) + \sigma a_{gs,ZF} (\alpha_{gs} T_{ZF,s}^4 - \epsilon_g T_{ZF,g}^4) + \sigma a_{w,in} (\alpha_{gw} T_w^4 - \epsilon_g T_{ZF,g}^4) \quad (18)$$

$$h_{gs} (T_{ZF,s} - T_{ZF,g}) + \sigma (\alpha_{gs} T_{ZF,s}^4 - \epsilon_g T_{ZF,g}^4) + \sigma \frac{(T_w^4 - T_{ZF,s}^4)}{\frac{1-\epsilon_w}{\epsilon_w} \frac{a_{gs,ZF}}{a_{w,in}} + \frac{1}{F_{ZF,w}} + \frac{1-\epsilon_c}{\epsilon_c}} =$$

$$\sum_j (-\Delta H)_j \eta_j t_{ZF,c} \rho_s r_j(C_s, T_{ZF,s}) \quad (19)$$

In Eq. (18), $a_{w,in}$ is in $m_{w,in}^2/m_{ZF}^3$ and $\hat{A}_{b,in}$ in $m_{b,in}^2/m_{ZF}^3$ and $U_{b,ZF}$ is only considered to be significant in the bayonet insert region. The pressure drop and heat transfer correlations as discussed in Sections 3 and 5 were used. Radiative heat transfer between the heated reactor tube wall and the ZoneFlow™ casing and absorption in the participating gas medium are accounted for in the energy Eqs. (18) and (19) [Minette, 2019]. Radiation was found to contribute 10-20% of the heat from the reactor tube to the reacting gas for low-pressure reforming for steel production applications [Minette and De Wilde, 2021], but contributes only on the order of 5%, in the conventional SMR process for hydrogen production at around 30 bar because of the higher gas density. σ is the Stefan-Boltzmann constant, $5.670373 \times 10^{-8} \text{ W.m}^{-2}.\text{K}^{-4}$, ϵ_g is the gas emissivity, α_{gw} and α_{gs} the gas absorptivity based respectively on the wall and casing temperatures, ϵ_w and ϵ_c , the emissivities of the tube wall and the casing materials, and $F_{ZF,w}$ the view factor of the ZoneFlow™ casing blades coated with catalyst. A value of 20 m^{-1} was used for the absorption coefficient of the process gas. In Eqs. (17) and (19), the reaction kinetics of Xu and Froment [1989] were adopted, accounting for the two Steam Methane Reforming reactions and the Water-Gas-Shift reaction and the details of the reaction mechanism. An active catalyst layer of $t_{ZF,c} = 80 \text{ }\mu\text{m}$ was considered, leading to calculated catalyst effectiveness factors, η_j , close to 1 for both steam reforming reactions [Minette et al., 2021]. Equations (16)-(19) are solved together with pressure drop Eqs. (1), (3)-(5) and the energy equation for the bayonet side, Eq. (13), and using the following inlet conditions:

$$\begin{aligned} z = 0: \quad & C_A = C_{A0} \\ & T_{ZF,g} = T_0 \\ & P = P_0 \end{aligned} \quad (20)$$

At the reactor tube wall, a typical industrial heat flux profile, as shown in Figure 8, is imposed with a mean heat flux of 85 kW/m^2 . Hence, for all cases simulated, the total heat input from the furnace is 333.79 kW per tube. The other operating conditions and the characteristics of the ZoneFlow™-bayonet reactor are summarized in Table 4.

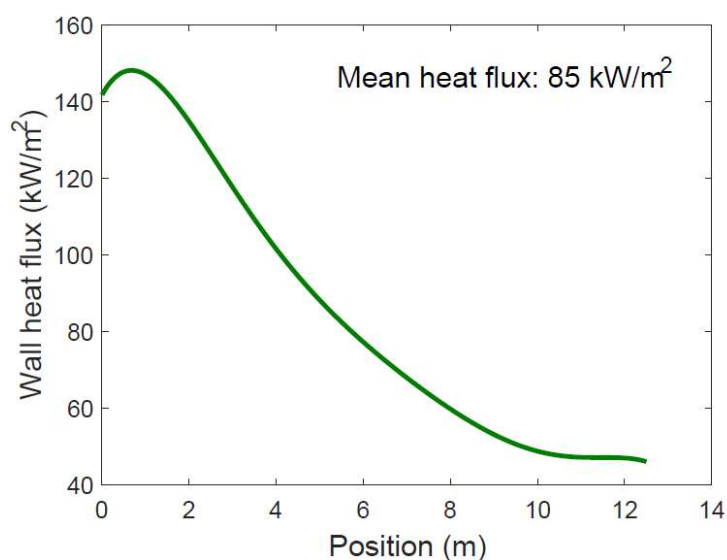


Figure 8. Heat flux profile imposed in the commercial scale SMR simulations.

Reactor design	
Length	12 m
Tube diameter	0.1 m
Reactor internals / structured catalyst	ZoneFlow™-bayonet reactor
Operating conditions	
Total feed rate	566 Nm ³ /hr
Inlet temperature	480 °C
Inlet pressure	33.8 bar
Feed composition	(mole fraction)
	CH ₄ 0.306
	CO ₂ 0.016
	CO 0
	H ₂ 0.066
	H ₂ O 0.611

Table 4. Operating conditions for the commercial scale SMR simulations.

Simulations were first carried out for a single-pass ZoneFlow™ reactor, i.e. without returning gas in the bayonet. Figure 9 shows the axial profiles of the tube skin temperature, reacting gas

temperature and methane conversion. With the relatively low mixed feed temperature, a methane conversion of 0.486 is reached and the syngas exits the ZoneFlow™ reactor at 806.9°C. The maximum tube skin temperature is 843°C.

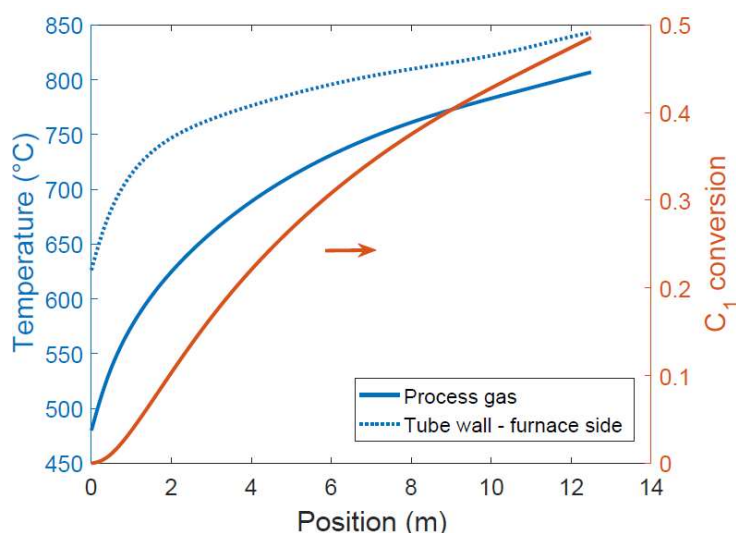


Figure 9. Axial profiles of the tube skin temperature, reacting gas temperature and methane conversion in a commercial scale single-pass ZoneFlow™ reactor for SMR. Imposed heat flux profile: see Figure 8. Operating conditions: see Table 4.

Simulations were then carried out with the ZoneFlow™-bayonet reactor configuration to compare the performance with that of the single pass ZoneFlow™ reactor and to optimize the bayonet insert diameter and length. The bayonet insert is always installed at the exit of the bayonet. Two parameters were optimized: the heat recovered from the return gas in the bayonet and the additional pressure drop caused by the bayonet insert. The mixed feed flow rate and temperature were kept constant at 566 Nm³/h and 480°C. A feed temperature lower than in conventional operation is used to take greater advantage of heat recovery from the return gas in the bayonet. The effect of the heat recovery from the return gas on the methane conversion and on the syngas exit temperature were analyzed. The risk of multiple steady states and instability, due to thermal feedback in the ZoneFlow™-bayonet reactor

configuration, was evaluated as shown in Appendix II. Even in the case of ideal heat recuperation, no multiple steady-states are possible with endothermic reactions, as in steam methane reforming.

Figure 10a shows the results obtained for the reference case without a bayonet insert, with only heat recovery from the empty bayonet tube. Axial profiles of the reactor tube skin temperature, inner wall temperature, reacting gas temperature (in the ZoneFlow™ reactor), return gas temperature in the bayonet and methane conversion are shown, as well as the pressure profile. With an empty bayonet, a total of 28.3 kW is recovered from the return gas exiting via the bayonet, corresponding to 7.82% of the total heat input to the ZoneFlow™ reactor, from the furnace and from the bayonet combined, or to 8.48% of the heat input from the furnace. A temperature drop in the bayonet of ca. 77.5°C is realized. The produced syngas exits the outer annulus with the ZoneFlow™ reactor at 825°C and the bayonet at 747.5°C. The maximum tube skin temperature is 861°C. The additional pressure drop in the empty bayonet tube is negligible. A methane conversion of 52.6% is reached, i.e. 8.2% increase in methane conversion compared to the single-pass ZoneFlow™ reactor. A comparison of key numbers for different cases is found in Table 5. Figures 10c,d and 10e,f show the profiles obtained with a 5 cm and 6 cm-diameter insert (as used in the experimental test campaigns), respectively, over the last 3 meters of the bayonet. The heat recovery improves by using a bayonet insert and with increasing bayonet insert diameter. The total amount of heat recovered from the return gas exiting via the bayonet increases to 39.4 kW with the 5 cm-diameter insert and to 49.4 kW with the 6 cm-diameter insert, that is, 10.56% and 12.88%, respectively, of the total heat input to the ZoneFlow™ reactor. The methane conversion increases to 54.6% and 56.1%, respectively. The temperature at which the produced syngas exits the outer annulus with the ZoneFlow™ reactor increases to 832°C and 838.3°C, respectively, and the temperature at which the return gas exits the bayonet decreases to 720.6°C and 693.6°C, respectively, so that the temperature drop in the bayonet increases to 111.4°C and 144.7°C, respectively. The maximum tube skin temperature is also affected and increases to 867°C and 874°C, respectively. Note that in industrial practice, the firing rate in the furnace or the mixed feed temperature can be reduced if the maximum allowable tube skin temperature is approached – for

simplicity of comparison, the heat flux from the furnace and the mixed feed temperature were kept constant in the simulations presented here.

The improved heat recovery from the return gas by means of a bayonet insert comes mainly at the cost of an increased pressure drop (Figure 10b,d,f). Whereas with a 5 cm-diameter, 3 m-long insert, the incremental pressure drop is negligible (< 0.1 bar) compared to the 1.13 bar pressure drop in the ZoneFlowTM reactor, the pressure drop increases to 1.96 bar with a 6 cm-diameter, 3 m long insert. The total pressure drop over the ZoneFlowTM-bayonet reactor is still acceptable for commercial application, however, as the pressure drop over the annular ZoneFlowTM reactor itself is ca. 40% lower than over a packed bed of conventional SMR catalyst pellets in the absence of a bayonet [Minette et al., 2021].

Simulations were carried out with a 3 m long bayonet insert and various insert diameters to optimize the heat recovery versus increase in pressure drop. Figure 11a shows the percentage of the total heat provided to the ZoneFlowTM reactor that is coming from the return gas in the bayonet and the total pressure drop over the ZoneFlowTM-bayonet reactor as a function of the bayonet insert diameter. Whereas the heat recovery increases quite linearly with the bayonet insert diameter, a non-linear increase of the pressure drop is observed – as expected from the pressure drop Eq. (5). A 5.4 cm-diameter, 3 m long insert gives a reasonable pressure drop with 11.3% of the total heat input to the ZoneFlowTM reactor provided by the return gas. The length of the 5.4 cm diameter insert was then varied to study the influence on the heat recovery and the pressure drop, as shown in Figure 11b. Whereas the pressure drop logically increases proportionally with the insert length, the incremental heat recovery decreases. This is the result of a decreasing temperature difference or driving force for heat transfer nearer the tip of the tube. From the profiles in Figure 11b, a 6 m long insert of 5.4 cm diameter seems effective. With this design, the additional pressure drop caused by the bayonet insert is less than 0.3 bar and the return gas in the bayonet provides 12.51% of the total heat input to the

ZoneFlow™ reactor. The methane conversion is 0.559. The syngas exits the ZoneFlow™ annular reactor at a temperature of 837.2°C and the temperature drop in the bayonet is 135.8°C.

Figures 11a and 11b show that in first instance, increasing the insert length is preferred over increasing the insert diameter to improve heat recovery from the return gas, as it comes at a lower incremental pressure drop. From a certain point on, however, not much heat recovery can be gained by further increasing the insert length and increasing the insert diameter is required. Note that the total pressure drop remains lower than the pressure drop for a packed bed of conventional SMR pellets in the absence of a bayonet for heat recovery.

With the optimized bayonet insert design, it is possible to reach the same methane conversion than with an empty bayonet, but with a lower imposed average heat flux from the furnace. Indeed, using the same heat flux profile as in Figure 8, a methane conversion of 0.526 can be reached with an average heat flux of 80 kW/m² instead of 85 kW/m², i.e. a reduction of 5.88%. In this case, the total heat input from the furnace is 314.16 kW and the return gas in the bayonet provides 45.7 kW, which corresponds to 12.7% of the total heat input to the ZoneFlow™ reactor. For a direct comparison of key numbers with other cases, reference is made to Table 5.

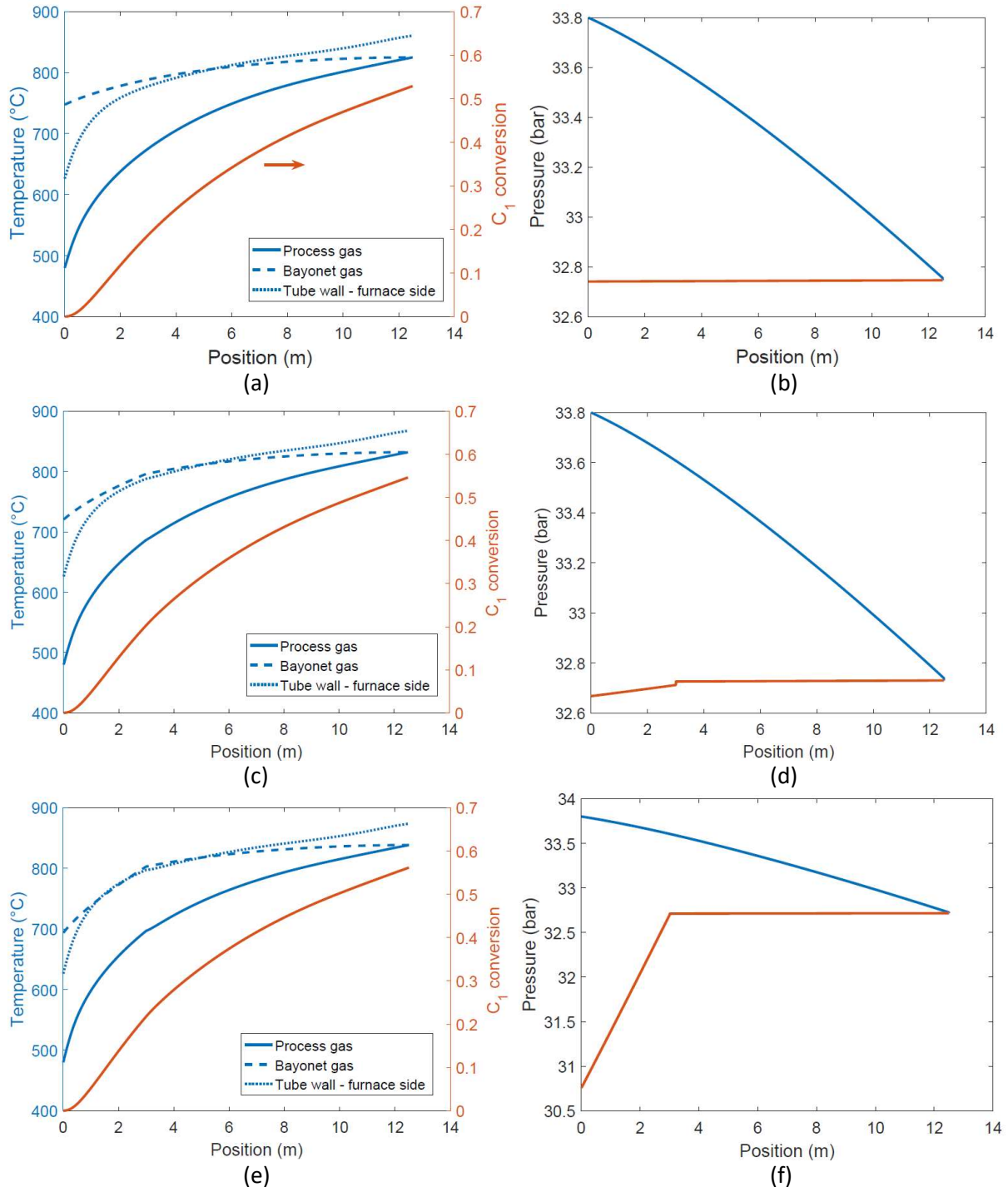
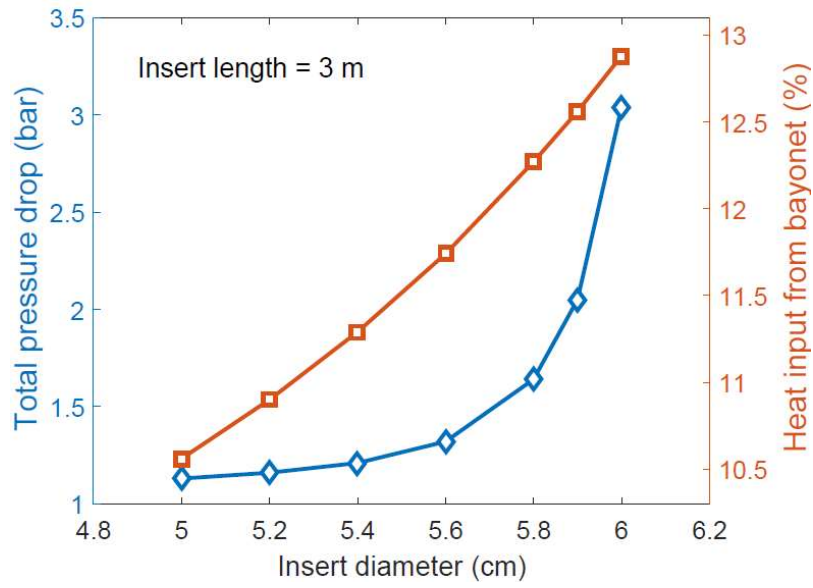
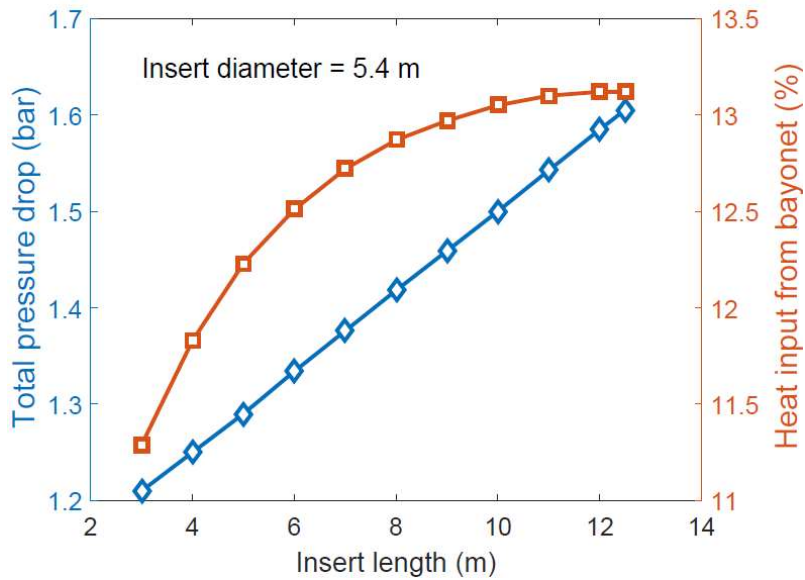


Figure 10. Axial in a commercial scale ZoneFlow™-bayonet reactor for SMR of the temperatures (gas reacting in the ZoneFlow™ reactor, return gas in the bayonet, reactor tube skin and inner wall), the methane conversion (a,c,e) and the pressure (b,d,f) when using (a,b) an empty bayonet (no insert), (c,d) a 3 m-long, 5 cm-diameter bayonet insert, and (e,f) a 3 m-long, 6 cm-diameter bayonet insert. Imposed heat flux profile: see Figure 8. Operating conditions: see Table 4.



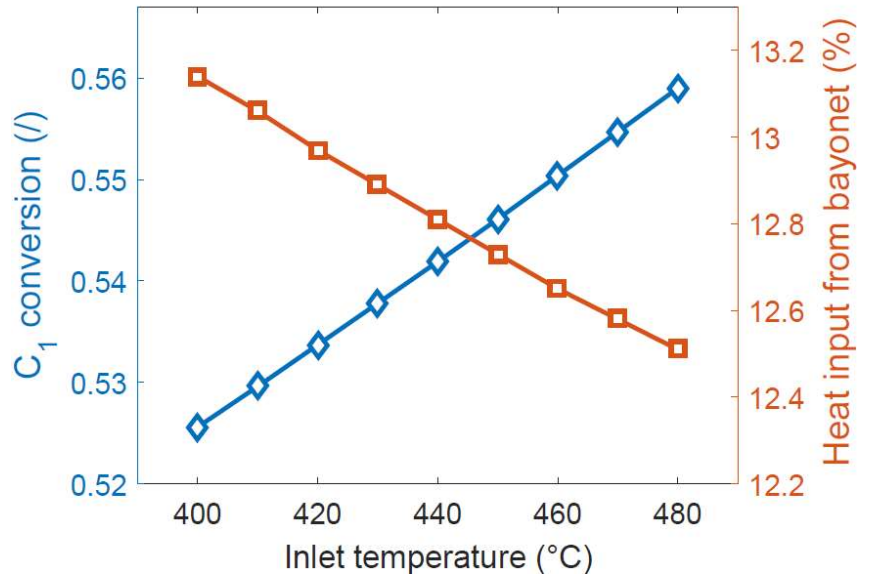
(a)



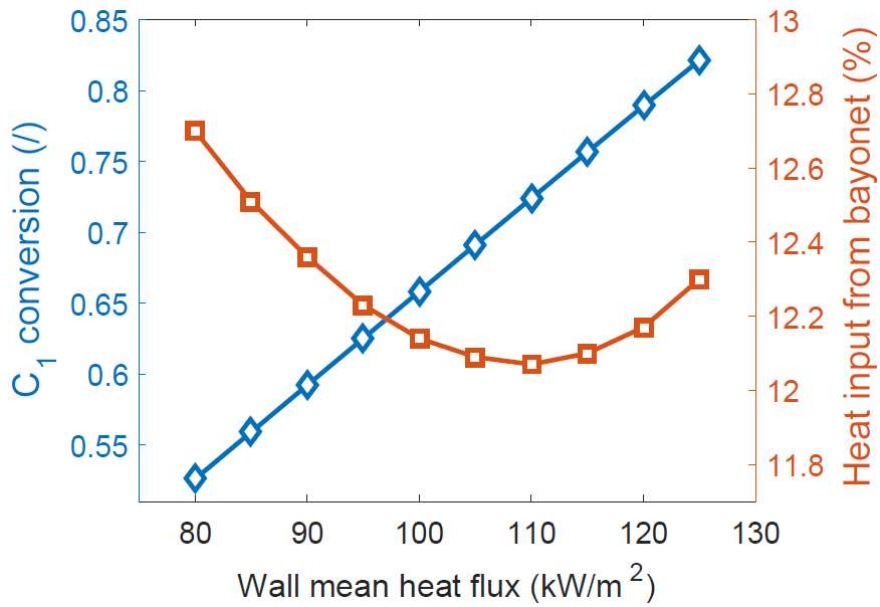
(b)

Figure 11. Optimization of the bayonet insert design for commercial scale SMR. Influence on the percentage heat to the ZoneFlow™ reactor coming from the return gas in the bayonet and on the pressure drop of (a) the insert diameter (3 m-long insert) and (b) the insert length (0.54 m-diameter insert) for the heat flux profile of Figure 8 and operating conditions of Table 4.

Further simulations were carried out with the optimized 6 m long, 5.4 cm diameter bayonet insert, varying the mixed feed temperature or the average heat flux from the furnace while maintaining the heat flux profile as shown in Figure 8. As shown in Figure 12a and Table 5, lowering the mixed feed temperature results in relatively more heat recovery from the return gas in the bayonet, but a lower methane conversion. At mixed feed temperatures of 480°C and 400°C, respectively, the % of the total heat to the ZoneFlow™ reactor coming from the return gas in the bayonet is 12.51% and 13.14%, the methane conversion 0.559 and 0.526. Figure 12b and Table 5 show that when increasing the average heat input from the furnace from 80 to 125 kW/m², the methane conversion steadily increases from 52.6 to 82.13%, the temperature drop in the bayonet increases from 130 to 192°C, and the maximum tube skin temperature increases from 857 to 1005°C, which is above typically applicable values. On the other hand, the relative heat recovery from the return gas in the bayonet first decreases from 12.7% to 12.07%, at an average furnace heat flux of 110 kW/m², and then increases again to 12.3%.



(a)



(b)

Figure 12. Sensitivity study of the operating conditions for commercial scale SMR. Influence on the methane conversion and on the percentage heat to the ZoneFlow™ reactor coming from the return gas in the bayonet of (a) the inlet temperature and (b) the average furnace heat flux, using a 6 m long, 5.4 cm diameter bayonet insert. Heat flux profile of Figure 8 (with varying average value in (b)) and operating conditions of Table 4.

Finally, a simulation was carried out with a 6 m long insert of 5.4 cm diameter, but in absence of air gap between the bayonet tube and the sliding spacers, assuming perfect contact or perforated spacers. In this case and as summarized in Table 5, 14.53% of the total heat input to the ZoneFlow™ reactor is provided by the return gas in the bayonet, compared to 12.51% with a 50 μm air gap. The methane conversion reaches a value of 0.573 instead of 0.559. The syngas exit temperature from the ZoneFlow™ reactor increases from 837.2°C to 843°C and the temperature drop in the bayonet increases from 135.8°C to 161°C. On the other hand, when increasing the air gap to 100 μm , 10.99% of the total heat input to the ZoneFlow™ reactor is seen to come from the return gas and the methane conversion reduces to 0.549. The syngas exit temperature from the ZoneFlow™ reactor decreases to 833°C, the temperature drop in the bayonet to 117.6°C.

Insert length (m)	Insert diameter (cm)	Air gap between tube and spacers (μm)	Mixed feed temperature ($^{\circ}\text{C}$)	Mean surface heat flux (kW/m^2)	ZF exit temperature ($^{\circ}\text{C}$)	Bayonet temperature drop ($^{\circ}\text{C}$)	Percentage total heat input to ZF reactor from return gas (%)	Percentage furnace heat recovered (%)	Methane conversion (%)
/	/	/	480	85	806.9	/	/	/	48.6
/	/	50	480	85	825	77.5	7.82	8.48	52.6
3	5	50	480	85	832	111.4	10.56	11.81	54.6
3	6	50	480	85	838.3	144.7	12.88	14.78	56.1
6	5.4	50	480	85	837.2	135.8	12.51	14.3	55.9
6	5.4	50	480	80	823.3	130.3	12.7	14.55	52.6
6	5.4	50	400	85	823.5	146.1	13.14	15.13	52.56
6	5.4	50	480	125	958.35	192.05	12.3	14.03	82.13
6	5.4	0	480	85	843	161	14.53	17.01	57.3
6	5.4	100	480	85	833	117.6	10.99	12.35	54.9

Table 5. Simulations of the commercial-scale ZoneFlowTM-bayonet reactor. Comparison of the syngas temperature at the exit of the annular ZoneFlowTM reactor, the temperature drop in the central bayonet tube, the percentage of total heat to the ZoneFlowTM reactor coming from the return gas in the bayonet, the percentage recovered furnace heat, and the methane conversion for various configurations (single pass, empty bayonet, bayonet with insert), designs and operating conditions. Heat flux profile of Figure 8 and operating conditions of Table 4.

7. Conclusions

The ZoneFlow™-bayonet reactor configuration combines the reduced pressure drop and improved heat transfer at the tube wall of the annular structured ZoneFlow™ reactor with the heat recovery of bayonet reactors to reduce the steam production and firing rate. Heat recovery is made more efficient by introducing an insert to create a short annulus within the bayonet tube near the inlet/outlet end of the tube to generate high velocity return gas flow close to wall of the bayonet tube. In the first part of the paper, experiments were carried out at commercial scale and at flow rates representative of commercial steam reforming conditions to model the pressure drop and heat transfer for commercial operation. The pressure drops contributed by the change in flow direction and entry into the bayonet, the inlet effect of the bayonet insert annulus, and the flow along that bayonet annulus were individually experimentally studied and modeled. Relatively good fit was found between the present work and the published equations for pressure drop in concentric annuli of Quarmby [1967]. Computational Fluid Dynamics simulations confirmed that the Dittus-Boelter [1930] equation accurately calculates the heat transfer between the return gas in the bayonet and the inside of the bayonet tube wall. The heat transfer between the gas reacting in the ZoneFlow™ reactor and the outside of the bayonet tube wall was then modeled from the experimental data. An insert giving a relatively small annulus was used inside the bayonet tube to ensure the main resistance for heat transfer between the return gas in the bayonet and the reacting gas was located on the outside of the bayonet tube.

In the second part of the paper, commercial scale ZoneFlow™-bayonet reactors were simulated to optimize the tradeoffs between heat recovery and pressure drop. With a 5.4 cm diameter, 6 m long insert, 12.51% of the total heat input to the ZoneFlow™ reactor came from the return gas, corresponding to 14.3% furnace heat recovery. Without a bayonet insert, only 7.82% of the total heat input to the ZoneFlow™ reactor came from the return gas in the bayonet. The additional pressure drop caused by the insert is less than 0.3 bar. The total pressure drop over the ZoneFlow™-bayonet reactor

also stays below the pressure drop over a packed bed of conventional SMR catalyst pellets without a bayonet. Greater heat recovery is possible at the expense of greater pressure drop. Increasing the insert length improves heat recovery with a relatively less increase in pressure drop than reducing the annular gap in the bayonet, but has its limitations. By decreasing the mixed feed temperature to the ZoneFlow™ reactor, heat recovery can be also improved, but the methane conversion is reduced. An increased furnace heat flux increases the methane conversion, while the percentage heat to the ZoneFlow™ reactor coming from the return gas first decreases and then again increases. The maximum allowable tube skin temperature can, however, be exceeded at too high furnace heat fluxes. By eliminating the air gap between the bayonet tube and the ZoneFlow™ reactor spacers, the percentage of total heat to the ZoneFlow™ reactor coming from the return gas in the bayonet can increase to 14.53%, corresponding to 17.01% of the heat provided by the furnace.

Appendix I: Computational Fluid Dynamics simulations validating the applicability of the Dittus-Boelter correlation for $\alpha_{b,in}$

Computational Fluid Dynamics (CFD) simulations were carried out to validate use of the Dittus-Boelter [1930] equation, Eq. (9), for the coefficient of heat transfer between the return gas in the bayonet insert region and the inside of the bayonet tube, $\alpha_{b,in}$. A Reynolds-Averaged Navier-Stokes (RANS) approach was adopted and Ansys Fluent was used for the simulations. To account for the turbulence, the standard $k-\varepsilon$ model with enhanced wall treatment was used [Lauder and Spalding, 1974; Fluent User Guide, 2020]. Simulations were carried out on a 6° sector of the annulus formed between the inside of the bayonet tube and the insert, imposing periodic boundary conditions. The grid was refined near the bayonet wall (Figure A1a) and a grid independency study was carried out. The final mesh used consisted of 11.3 Mcells. Simulations were carried out feeding air at 500K at various flow rates in the range of $u_{s,bi} = 50 - 250 \text{ m}^3/\text{m}_{bi}^2\text{s}$, imposing a bayonet wall temperature of 300K. Figure A1b shows example contour plots of the temperature in the annulus between the bayonet tube and the bayonet

insert at the mid-length of the insert and at the outlet of the insert for an air flow rate of $u_{s,bi} = 150 \text{ m}_g^3/\text{m}_{bi}^2\text{s}$.

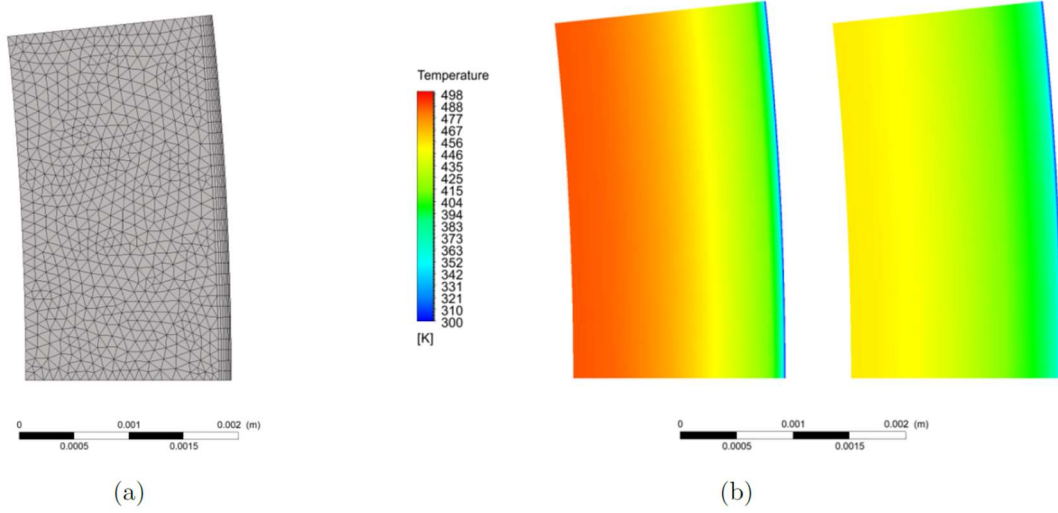


Figure A1. CFD simulations of the experimentally used bayonet insert configuration for the verification of the Dittus-Boelter [1930] equation for heat transfer between two concentric annuli. (a) Computational mesh; (b) Calculated temperatures in a transverse cross section at the mid-length of the bayonet insert (left) and at the exit of the bayonet insert region (right) – simulation at $u_{s,bi} = 150 \text{ m}_g^3/(\text{m}_{bi}^2\text{s})$. Dimensions: see Table 1.

To calculate the heat transfer coefficient for comparison with the Dittus-Boelter correlation, axial profiles of the cross-sectional averaged temperature were used. A comparison between the values of $\alpha_{b,in}$ obtained by the CFD simulations and calculated using the Dittus-Boelter correlation is shown in Figure A2. A good fit is observed in a relatively wide flow rate range, justifying the use of the Dittus-Boelter equation, Eq. (9), for the calculation of $\alpha_{b,in}$, allowing a more limited number of parameters to be estimated from the heat transfer measurements to b_1 and b_2 in the correlation for $\alpha_{b,ZF}$, Eq. (10).

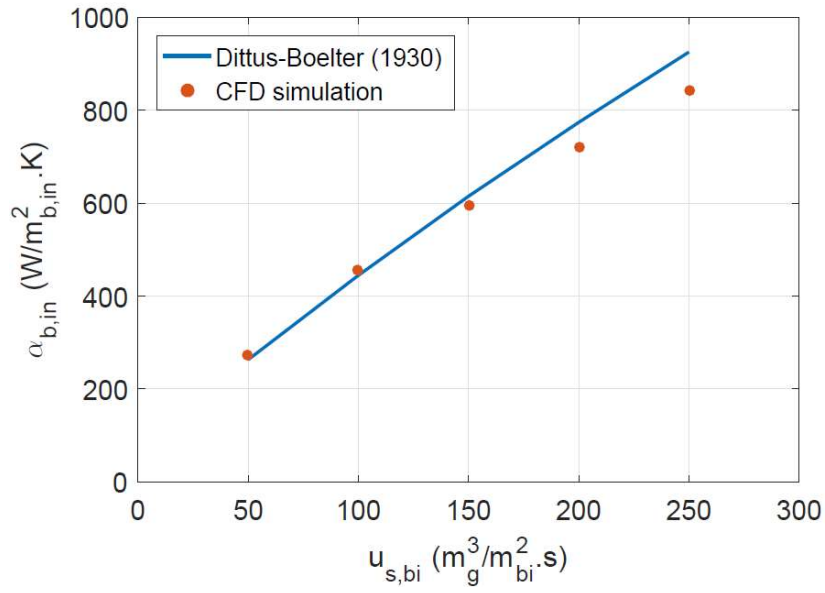


Figure A2. Coefficient of heat transfer between the gas in the bayonet insert region and the inside of the bayonet tube versus gas flow rate. Comparison of values calculated by means of CFD with those obtained by the Dittus-Boelter [1930] equation for the experimentally tested bayonet insert configuration. Dimensions: see Table 1.

Appendix II: Analysis of the risk of multiple steady-states and stability of the ZoneFlowTM-bayonet reactor configuration

The risk of existence of multiple steady states due to thermal feedback in the ZoneFlowTM-bayonet reactor configuration is investigated. A gradual increase of the temperature in the ZoneFlowTM reactor is considered. The analysis is based on the worst case in terms of thermal feedback, that is, where heat transfer between the return gas in the bayonet and the gas in the annular ZoneFlowTM reactor is infinitely fast so that the temperature profile in the bayonet closely follows the temperature profile in the reactor as shown in Figure A3.

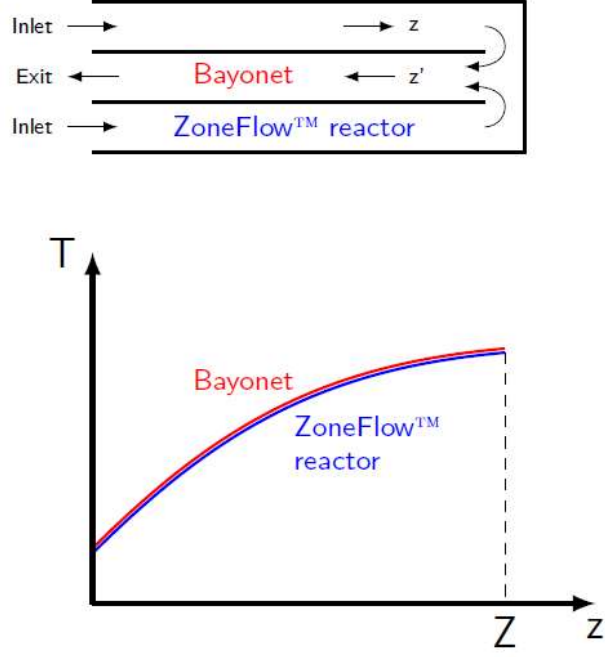


Figure A3. Schematic representation of the ZoneFlow™-bayonet reactor operation as considered for the verification of the existence of multiple steady states due to thermal feedback and the related stability analysis. Ideal heat recovery was assumed as worst case scenario in terms of thermal feedback.

The energy equation for the ZoneFlow™ reactor side is written:

$$\frac{\dot{m}c_P}{\Omega} \frac{\partial T}{\partial z} = r_A \rho_B (-\Delta H) + U_{f,ZF} \frac{\pi d_t}{\Omega} (T_f - T) + U_{ZF,b} \frac{\pi d_b}{\Omega} (T_b - T) \quad (\text{A1})$$

The energy equation for the bayonet side is:

$$\frac{\dot{m}c_P}{\Omega_b} \frac{\partial T_b}{\partial z'} = U_{ZF,b} \frac{\pi d_b}{\Omega_b} (T - T_b) \quad (\text{A2})$$

or equivalently:

$$\dot{m}c_P \frac{\partial T_b}{\partial z} = U_{ZF,b} \pi d_b (T_b - T) \quad (\text{A3})$$

Substituting (A3) in (A1) leads to:

$$\frac{\dot{m}c_P}{\Omega} \frac{\partial T}{\partial z} = r_A \rho_B (-\Delta H) + U_{f,ZF} \frac{\pi d_t}{\Omega} (T_f - T) + \frac{\dot{m}c_P}{\Omega} \frac{\partial T_b}{\partial z} \quad (\text{A4})$$

Assuming perfect heat recovery (Figure A3), $\frac{\partial T_b}{\partial z} = \frac{\partial T}{\partial z}$, so that no net heat is evacuated from a control volume in the reactor by the flow and Eq. (A4) reduces to:

$$r_A \rho_B (-\Delta H) = U_{f,ZF} \frac{\pi d_t}{\Omega} (T - T_f) \quad (\text{A5})$$

or: $Q_R = Q_F$ (A6)

where both sides are negative and with Q_F the heat input, provided by the furnace, and Q_R the heat consumed by the reactions.

In steady state operation, the local thermal equilibrium has to be satisfied at any position in the reactor. Note that Eq. (A5) is of the same form as the solid phase heat equation in a heterogeneous fixed bed reactor model – the possibility of multiple steady states in case of exothermic reactions are well known. With endothermic reactions, however, no multiple steady states are possible, as illustrated in Figure A4 in which Q_R and Q_F are plotted as a function of the reactor temperature T .

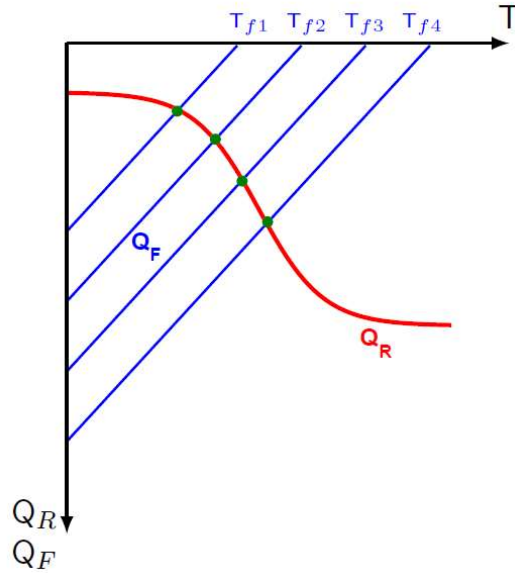


Figure A4. Q_R and Q_F – as defined in Eq. (A5) and (A6) – as a function of the reactor temperature T to verify the possibility of multiple solutions of Eq. (A5) (multiple steady states) and stable operation. Worst case scenario in terms of thermal feedback considered.

No multiple steady states are found in the ZoneFlow™-bayonet Reactor in the considered worst case in terms of thermal feedback with the slope $\partial Q_F/\partial T$ always larger than $\partial Q_R/\partial T$. The latter implies stable operation. E.g. an increase of the temperature around a steady state solution point (at given T_f) will result in increased heat consumption by the (endothermic) reactions and reduced heat supply by the furnace (at constant T_f), so that the temperature will decrease again to the original value. Similarly, a decrease of the temperature around a steady state solution point will result in decreased heat consumption by the reactions and increased heat supply by the furnace, so that the temperature will increase again to the original value.

References

- Air Liquide. SMR-X™ - Production d'hydrogène avec zéro vapeur: Produire de l'hydrogène sans exporter de la vapeur. <https://www.engineering-airliquide.com/fr/smr-x-production-hydrogene-zero-vapeur> (2020).
- Corgnale C., Shimpalee S., Gorenssek M.B., Satjaritanun P., Weidner J.W., Summers W.A. Numerical modeling of a bayonet heat exchanger-based reactor for sulfuric acid decomposition in thermochemical hydrogen production processes. *International Journal of Hydrogen Energy* 42(32), p. 20463-20472 (2017).
- Damiani L., Montecucco M., Prato A.P. Conceptual design of a bayonet-tube steam generator for the ALFRED lead-cooled reactor. *Nuclear Engineering and Design* 265, p. 154-163 (2013).
- De Wilde J., Froment G.F. Computational Fluid Dynamics in chemical reactor analysis and design: Application to the ZoneFlow™ reactor for methane steam reforming. *Fuel* 100, p. 48-56 (2012).
- De Wilde J., Froment G.F. Modeling of dual-zone structured reactors for natural gas steam reforming. *Industrial & Engineering Chemistry Research* 52, p. 14055-14065 (2013).
- Dittus, F.W., Boelter, L.M.K. Heat Transfer in Automobile Radiators of the Tubular Type. University of California Press, Berkeley, University of California Publications on Engineering, Vol. 2, p. 443-461 (1930). Reprinted in *Int. Commun. Heat Mass* 12, p. 3-22 (1985).
- Fluent User's Guide. Ansys (2020).
- Froment G.F., Bischoff K.B., De Wilde J. *Chemical Reactor Analysis and Design*, 3th ed., Wiley (2010).
- Halder Topsoe. Bayonet reformer (SMR-b). <https://www.topsoe.com/products/equipment/bayonet-reformer-smr-b> (2020).

Launder B.E., Spalding D.B. The numerical computation of turbulent flows. *Computer Methods in Applied Mechanics and Engineering* 3(2), p. 269–289 (1974).

Minette F. Multi-scale modeling and design of a structured catalytic reactor for bi-reforming of methane. PhD thesis, UCLouvain, Belgium (2019).

Minette F., Calamote de Almeida L., Ratan S., De Wilde J. Pressure drop and heat transfer of ZoneFlow™ structured catalytic reactors and reference pellets for Steam Methane Reforming. *Chemical Engineering Journal*, 12808 (2021), <https://doi.org/10.1016/j.cej.2020.128080>.

Quarmby A. An Experimental Study of Turbulent Flow through Concentric Annuli. *International Journal of Mechanical Sciences* 9(4), p. 205-221 (1967a).

Quarmby A. On the use of the Preston Tube in concentric annuli. *The Aeronautical Journal* 71(673), p. 47-49 (1967b).

Ralston M.P., Feinstein J.J. Steam methane reformer system and method of performing a steam methane reforming process. US20160002035A1 (2015).

Saudemont E. Hydrogène : Air Liquide va investir 80 M€ dans une unité SMR de « nouvelle génération ». *Pétrole & Gaz: Énergies nouvelles*, April 18 (2018), <http://www.petrole-et-gaz.fr/hydrogene-air-liquide-va-investir-80-me-dans-une-unite-smr-de-nouvelle-generation-11275/>.

Xu J., Froment G.F. Methane Steam Reforming, Methanation and Water-Gas Shift: I. Intrinsic kinetics. *AIChE Journal* 35, p. 88-96 (1989).